

# Micro-video Tagging via Jointly Modeling Social Influence and Tag Relation

Xiao Wang  
scz.wangxiao@gmail.com  
Shandong University

Tian Gan\*  
gantian@sdu.edu.cn  
Shandong University

Yinwei Wei  
weiyinwei@hotmail.com  
National University of Singapore

Jianlong Wu\*  
jlwuhust@gmail.com  
Harbin Institute of Technology  
(Shenzhen) & Shandong University

Dai Meng  
daimeng@kuaishou.com  
Kuaishou Technology

Liqiang Nie  
nieliqiang@gmail.com  
Harbin Institute of Technology  
(Shenzhen)

## ABSTRACT

The last decade has witnessed the proliferation of micro-videos on various user-generated content platforms. According to our statistics, around 85.7% of micro-videos lack annotation. In this paper, we focus on annotating micro-videos with tags. Existing methods mostly focus on analyzing video content, neglecting users' social influence and tag relation. Meanwhile, existing tag relation construction methods suffer from either deficient performance or low tag coverage. To jointly model social influence and tag relation, we formulate micro-video tagging as a link prediction problem in a constructed heterogeneous network. Specifically, the tag relation (represented by tag ontology) is constructed in a semi-supervised manner. Then, we combine tag relation, video-tag annotation, and user follow relation to build the network. Afterward, a better video and tag representation are derived through Behavior Spread modeling and visual and linguistic knowledge aggregation. Finally, the semantic similarity between each micro-video and all candidate tags is calculated in this video-tag network. Extensive experiments on industrial datasets of three verticals verify the superiority of our model compared with several state-of-the-art baselines.

## CCS CONCEPTS

• Information systems → Document representation.

## KEYWORDS

Micro-video Tagging; Behavior Spread; Ontology Construction

## 1 INTRODUCTION

The last decade has evidenced the prosperity of micro-videos in User-Generated Content (UGC) platforms. To strengthen the applications like searching and recommendation [25, 34, 35], tags are widely-used to summarize micro-videos. Considering the fact that users may not add sufficient tags when uploading micro-videos, tagging has hence become an expensive routine for operation teams on UGC platforms. According to the statistics over 600 million videos collected from Kuaishou platform, around 85.7% of them have no tags at all. In order to generate tags with minimal human efforts, automatic micro-video tagging has drawn considerable attention from industrial and academic communities. Most existing methods formulate video tagging as a multi-label classification problem.

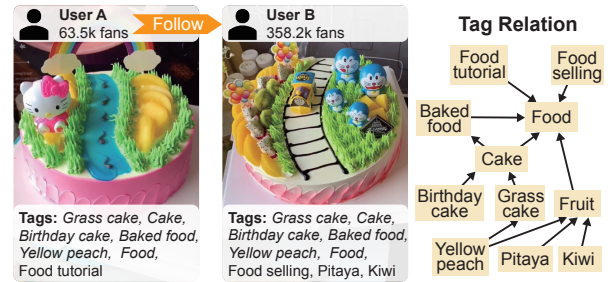


**Figure 1: Example of social influence and tag relation. Social influence: user A is a follower of B, and imitates user B to create a video with similar tags (illustrated in *italics*).**

Basic methods leverage information from video content and descriptions for tagging [15, 36]. Sophisticated methods leverage extra information, such as tag graph [3, 9, 14, 38], query log [21], user behavior [2], and user profile [11, 33] to assist tagging.

However, users' social influence and tag relation are rarely discussed, which could have played a pivotal role. On one hand, users' social influence is crucial since user may imitate their social network neighbors to create similar micro-videos, especially on UGC platforms because users are not only content creators but also consumers. Taking Fig. 1 as an example, user B produces a micro-video about a “grass cake”, and then the follower, user A, imitates this video to produce a similar one with almost the same set of tags. Such imitation phenomenon in the social network, namely **Behavior Spread** [1], can enhance tagging performance if correctly modeled. On the other hand, tag relation is reflected by a **tag ontology**, which is often represented as a Directed Acyclic Graph (DAG) composed of tags with *is\_subtopic\_of* relations. Tag ontology facilitates tagging by providing external knowledge from three aspects: (i) tag dependencies [32, 38], (ii) top-down knowledge transfer [11], and (iii) bottom-up semantics abstraction [22].

To incorporate users' social influence and tag relations, we build a heterogeneous user-video-tag network. This heterogeneous graph neural network is then used to derive a better video and tag representation. Consequently, we are able to measure the video-tag similarity to get tagging results. There are still challenges for the above approach: **C1: Behavior Spread modeling**. We need to propose an effective model to filter irrelevant information for Behavior Spread modeling, since not all micro-videos are created through imitation. **C2: Visual-linguistic knowledge aggregation**. There are two sources of knowledge for learning a tag representation: visual

\*Corresponding authors: Tian Gan and Jianlong Wu.

knowledge from videos and linguistic knowledge from relevant tags in the tag ontology. Existing aggregation methods [32, 38] that apply direct aggregation approaches like vector concatenation or attention mechanism are sub-optimal due to the ignorance of the redundancy in common knowledge. Concretely, concatenation duplicates the common knowledge, and attention mechanism tends to over concern the unique knowledge [13, 19, 28]. **C3: Tag ontology construction.** Most of the methods [11, 32] acquire the desired tag ontology from existing open knowledge bases. However, because video content in UGC platforms changes very fast, open knowledge bases can cover only a portion of tags. Other methods [3, 6] attempt to build the tag ontology from tag statistics. These methods are rule-based and thus lack accuracy.

To solve C3, we construct a tag ontology using semi-supervised classification based upon hand-crafted features. After that, we design an adversarial aggregated graph transformer network (RADAR) to propagate information over the entire graph for a better representation of each micro-video and tag node. RADAR is a heterogeneous Graph Neural Network (GNN) composed of a Gated Graph Transformer (GGT) and an Adversarial Aggregation Network (AAN). GGT aims to tackle C1 by aggregating information from neighbors, and filtering irrelevant information. To cope with C2, AAN is applied to aggregate visual and linguistic knowledge by removing the redundant information while keeping the complementary. Finally, we compute the semantic similarity between a given micro-video and all candidate tags as our predictions. To justify our model, we conduct extensive experiments over large-scale real-world datasets. The experimental results demonstrate the effectiveness of GGT and ANN, and our methods are consistently superior to several start-of-the-art baselines.

In summary, the contributions of this work are threefold:

- We construct a dataset of 450,000 micro-videos with their creators' social network in a UGC platform, and our experiments show that social network can benefit video tagging. To the best of our knowledge, this is the first work on modeling users' social influence towards micro-video tagging.
- We propose a semi-supervised manner to build a tag ontology, outperforming existing methods with little human effort.
- We design RADAR, a heterogeneous GNN composed of GGT and AAN to jointly model users' social influence and tag relation in an end-to-end manner. RADAR outperforms cutting-edge methods with a clear margin in real-world datasets. Our code is available<sup>1</sup>.

## 2 RELATED WORK

### 2.1 Video Tagging

Video tagging aims to find keywords that can describe the core content of a video. All methods can be categorized into two types based on the information they use. **Basic methods** leverage information only from video content: textual, visual, and audio. There are two sub-types. Key-phrase extraction methods extract tags from video descriptions [23, 24, 37], and rank them according to their relevance with core semantics [10, 24]. Multi-label classification methods assign tags from a predefined word set to videos [4, 15, 36]. **Sophisticated methods** leverage extra information besides video content, such as tag graph with knowledge [3, 9, 14, 38], query log

[21], user behavior [2], and user profile [11, 33]. Among all the above extra information, tag graph has attracted the most attention. Generally, the tag graph is built either from tag co-occurrence [3, 32, 38] or common knowledge bases [11, 12, 32]. However, the former can only provide statistical relations, and the latter has low tag coverage. Contrary to the tag graph, social network information (user follow, specifically) has not been touched in video tagging.

### 2.2 Heterogeneous Graph Neural Network

Heterogeneous networks are graphs with more than one meta-paths. Heterogeneous graph neural networks are widely applied to derive a better node representation for them [5, 17, 39, 40]. For example, Wang *et al.* [31] proposed a method which is based on two-level attention. Concretely, node-level attention measures the importance of neighbors within each meta-path, and semantic-level attention measures the importance of different meta-paths. Hu *et al.* [8] proposed a method in which node and edge-type dependent parameters are used to parameterize the graph transformer network of each meta-path. Lv *et al.* [20] proposed a method to demonstrate that a simple graph attention network combined with three well-known techniques can outperform all previous models.

## 3 PROBLEM FORMULATION

We formulate micro-video tagging as a link prediction problem on a video-tag network  $G(\mathcal{V}, \mathcal{E})$ .  $\mathcal{V}$  is the node set composed of videos and tags, and  $\mathcal{E}$  is the edge set. Note that video tagging with graphical data can also be formulated as a knowledge graph embedding problem [9]. However, such formulation only supports transductive learning, and is unable to handle new videos.

For each node  $u \in \mathcal{V}$ , we denote its initial representation as  $h^0(u) \in \mathbb{R}^d$ , where  $d$  is the size of hidden dimension. For tag node,  $h^0$  comes from the sum of word embedding and learnable embedding. For video node,  $h^0$  comes from aggregated frame embedding. Given  $h^0$  and  $G$ , our RADAR model, a  $L$ -layer heterogeneous GNN, can derive a better node representation  $h^L \in \mathbb{R}^d$ :

$$h^L = \text{RADAR}(h^0, G). \quad (1)$$

Based on this representation, we predict the confidence score  $\hat{y}(v, t) \in \mathbb{R}$  that micro-video  $v \in \mathcal{V}_{\text{video}}$  has tag  $t \in \mathcal{V}_{\text{tag}}$ :

$$\hat{y}(v, t) = \text{Sigmoid}\left(h^L(v) \cdot [h^L(t)]^T\right). \quad (2)$$

## 4 METHODOLOGY

Our overall framework is summarized in Fig. 2. We first propose a semi-supervised classification method to build a tag ontology, solving the ontology construction challenge. We then build the heterogeneous video-tag network for jointly modeling social influence and tag ontology. Afterward, we design the adversarial aggregated graph transformer network (RADAR) to derive a better video and tag representation. The two components of RADAR solve Behavior Spread modeling and visual-linguistic knowledge aggregation challenges respectively. Finally, we estimate the semantic similarity between a micro-video and all tags as our predictions.

### 4.1 Tag Ontology Construction

In this subsection, we construct the tag ontology, a graph composed of tags and *is\_subtopic\_of* relations. It is naturally a Directed Acyclic Graph (DAG), because a cycle made of *is\_subtopic\_of* relations

<sup>1</sup><https://github.com/SCZwangxiao/RADAR-MM2022.git>

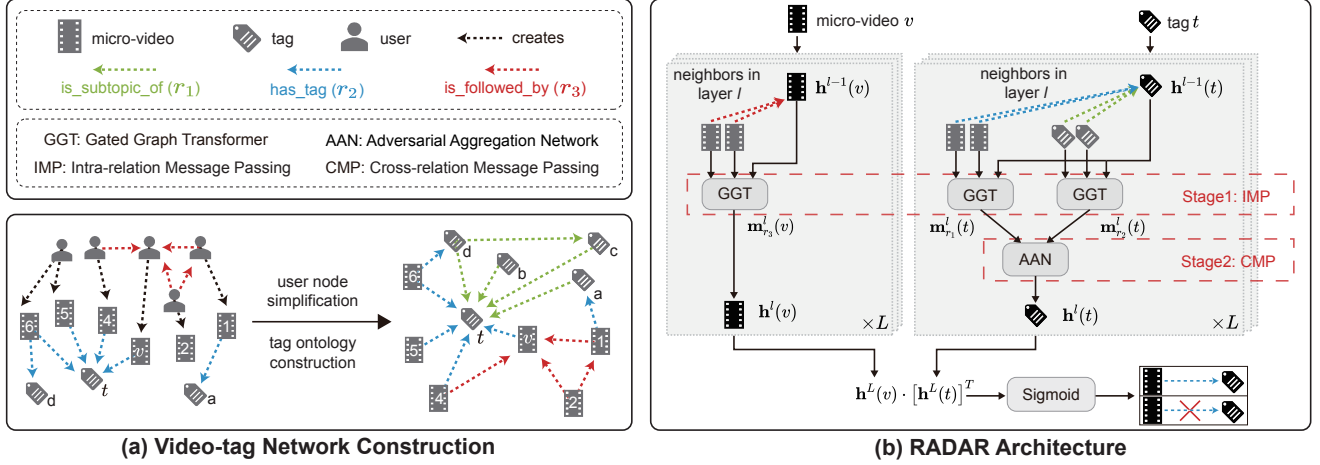


**Figure 2: Method overview.** (a) The video-tag network is built from the raw data composed of users and their micro-videos annotated with tags. (b) The GNN propagation of our RADAR network in each layer has two stages.

would cause a paradox. Ontology construction consists of two steps: subtopic discovery and DAG construction, as summarized in Fig. 3. In subtopic discovery, we discover subtopic relations among tags using semi-supervised classification based on hand-crafted features. These features are derived from tag statistics in video-tag annotations so that we can cover all tags. This step will produce a DAG violated graph. Following that, graphical constraints are imposed to derive a DAG as the final tag ontology.

**4.1.1 Subtopic Discovery.** We presume that *if two tags have subtopic relations, they will co-occur in at least one micro-video*. Based on this, we formulate subtopic discovery as a binary classification problem on co-occurred tags. Formally, for each co-occurred tag pair  $(u, v)$ ,  $u, v \in \mathcal{V}_{\text{tag}}$ , we predict their subtopic score  $r(u, v)$ :

$$r(u, v) = g(k(u, v)), \quad (3)$$

$$r(u, v) = \begin{cases} 1 & \text{if } v \text{ is a subtopic of } u, \\ 0 & \text{if no relationship between } u \text{ and } v, \end{cases} \quad (4)$$

where  $g(\cdot)$  can be an arbitrary classifier,  $k(u, v) \in \mathbb{R}^{d_r}$  is our hand-crafted features, and  $d_r$  is the dimension of feature. The features are designed to reflect the following two properties between tags:

**Semantic overlap** refers to the overlap of meaning between two tags. If two tags  $u$  and  $v$  have subtopic relations, they must have semantic overlap. We measure the semantic overlap using Point-wise Mutual Information  $\text{PMI}(u, v) \in \mathbb{R}$ :

$$\text{PMI}(u, v) = \log \left( \frac{p(u, v)}{p(u)p(v)} \right), \quad (5)$$

and Point-wise Kullback-Leibler divergence  $\text{PKL}(u, v) \in \mathbb{R}$ :

$$\text{PKL}(u, v) = p(u, v) \log \left( \frac{p(u, v)}{p(u)p(v)} \right), \quad (6)$$

where  $p(u, v)$  is the probability that  $u, v$  occur in the same micro-video, and  $p(u), p(v)$  are the occurrence probability of  $u, v$ , respectively. Compared with PMI, PKL is less biased towards the rare-occurred tags due to the additional  $p(u, v)$ .

**Semantic broadness** means the broadness of tag meaning. Broader semantics indicates a higher level in tag ontology (e.g., “food” has

broader semantics than “cake”). We measure it using two features. One is tag transfer probability  $p(u|v) \in \mathbb{R}$  from  $v$  to  $u$ :

$$p(u|v) = \frac{|\text{videos that have tag } u \text{ and } v|}{|\text{videos that have tag } v|}. \quad (7)$$

Intuitively, the larger  $p(u|v)$  is, the more likely that  $v$  is a subtopic of  $u$ . For example, given that tag “cake” is a subtopic of “food”, and “cake” is used, it will be very likely to see “food” as well (i.e., large  $p(\text{food}|\text{cake})$ ). Empirically, this probability has proven to be effective in industrial concept mining system [16]. The other feature is tag entropy  $H(u) \in \mathbb{R}$ :

$$H(u) = - \sum_w p(u|w) \log(p(u|w)). \quad (8)$$

Intuitively, a tag with higher  $H(u)$  has more and stronger inbound tag transfers from others, indicating a higher level in tag ontology.  $H(u)$  is also used by FBVO [6] to derive visual ontology.

With the semantic overlap and broadness features above, we can define our hand-crafted feature  $k(u, v)$  containing six basic features:  $p(u|v), p(v|u), H(u), H(v), \text{PMI}(u, v), \text{PKL}(u, v)$ , and two second order features:  $\log(p(u|v)/p(v|u)), \log(H(u)/H(v))$ . Based upon these, the classification in Eqn. (3) is in a semi-supervised manner. Concretely, the labels come from a small portion of the co-occurred tag pairs. Meanwhile, the features can be computed from all co-occurred tags to leverage information in unlabeled data.

For each tag pair  $(u, v)$ , we can estimate the confidence score of  $v$  being a subtopic of  $u$ :  $\hat{r}(u, v)$ . We keep those tag pairs whose  $\hat{r}$  are larger than a threshold  $\delta_r$ , and link them into a directed graph.

**4.1.2 DAG Construction.** Since not all predictions are correct, there will be DAG violations definitely, as exemplified in Fig. 3(b). Thus, we impose graphical constraints to derive the final DAG.

As illustrated in Fig. 3(c), we first sort all tags according to their entropy  $H$  in descending order. Considering higher entropy means a higher level in tag ontology, we then keep *is\_subtopic\_of* relations only from tags with lower entropy to higher ones. Afterward, the sorted tag list can be seen as the topological sorting of a DAG, which can be our tag ontology. Note that there might be isolated components, because lots of edges are filtered when we keep  $\hat{r}(u, v) > \delta_r$ .

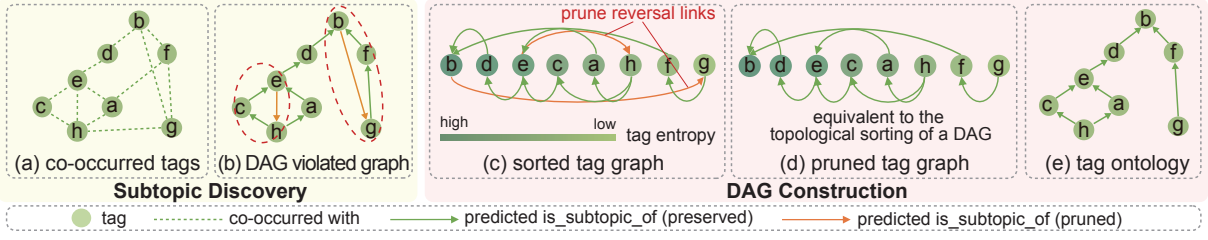


**Figure 3: Tag Ontology Construction.** (a)(b)  $Is\_subtopic\_of$  relations are discovered, and form a DAG violated graph. (c) All tags are sorted, and then the reversal links are pruned. (d)(e) The pruned tag graph is equivalent to a DAG, which is our tag ontology.

in subtopic discovery. For those components, we relax the constraint until they are not isolated or  $\hat{r}(u, v) < \epsilon_r$ , and link the remaining isolated ones to the tag with the highest entropy.

## 4.2 Video-tag Network

We build a directed heterogeneous video-tag network to incorporate social network and tag ontology, as shown in Fig. 2(a).

Our raw data is composed of users, micro-videos, and tags along with two relations: *has\_tag* and *is\_followed\_by*. The latter provides a clue about Behavior Spread.

We first simplify the raw data by deleting user nodes, and letting their created videos inherit *is\_followed\_by* relations. Concretely, if user<sub>A</sub> is followed by user<sub>B</sub>, then all user<sub>A</sub>'s videos are followed by user<sub>B</sub>'s videos. Note that we only preserve the *is\_followed\_by* relations pointing from previously-uploaded videos to newly-uploaded ones, because only old videos can influence new ones. After simplification, we incorporate the *is\_subtopic\_of* relations from the constructed tag ontology to get the video-tag network.

Formally, we denote the micro-video set as  $\mathcal{V}_{\text{video}}$  and tag set as  $\mathcal{V}_{\text{tag}}$ . They form the node set  $\mathcal{V} = \mathcal{V}_{\text{video}} \cup \mathcal{V}_{\text{tag}}$ . For convenience, we denote the three relations *is\_subtopic\_of*, *has\_tag*, and *is\_followed\_by* as  $r_1$ ,  $r_2$ , and  $r_3$ , respectively. Their corresponding relation sets are  $\mathcal{E}_{r_1}$ ,  $\mathcal{E}_{r_2}$ ,  $\mathcal{E}_{r_3}$ , respectively. They form the edge set  $\mathcal{E} = \mathcal{E}_{r_1} \cup \mathcal{E}_{r_2} \cup \mathcal{E}_{r_3}$ .

## 4.3 RADAR Architecture

**4.3.1 Overall RADAR Architecture.** To derive a better video and tag representation, we design RADAR, an  $L$  layer graph neural network. Considering that tag nodes have two types of inbound edges, while video nodes have only one, we apply different GNN propagation strategies to them. Concretely, we divide propagation into two stages: *intra-relation message passing* for both video and tag nodes and *cross-relation message aggregation* for tag nodes only. Correspondingly, each GNN layer in RADAR has two components: **Gated Graph Transformer (GGT)** and **Adversarial Aggregation Network (AAN)**, as illustrated in Fig. 2(b).

In the *intra-relation message passing* stage, GGT is applied for both tag and video nodes to derive message information propagated from their neighbors. Formally, video  $v$  receives message  $m_{r_3}^l(v) \in \mathbb{R}^d$  passed from its  $r_3$  neighbors:

$$m_{r_3}^l(v) = \text{GGT} \left( h^{l-1}(v), \left\{ h^{l-1}(s) \mid s \in \mathcal{N}_{r_3}^l(v) \right\} \right), \quad (9)$$

and video representation is updated by:

$$h^l(v) = m_{r_3}^l(v), \quad (10)$$

where the superscript  $l$  denotes the ( $l$ )-th layer,  $h^l(v) \in \mathbb{R}^d$  is the output representation of node  $v$ , and  $\mathcal{N}_{r_3}^l(v)$  are node  $v$ 's neighbors of  $r_3$  relations. Meanwhile, tag  $t$  receives messages  $m_{r_1}^l(t)$ ,  $m_{r_2}^l(t) \in \mathbb{R}^d$  passed from its  $r_1$  and  $r_2$  neighbors, respectively:

$$\begin{cases} m_{r_1}^l(t) = \text{GGT} \left( h^{l-1}(t), \left\{ h^{l-1}(s) \mid s \in \mathcal{N}_{r_1}^l(t) \right\} \right), & (11) \\ m_{r_2}^l(t) = \text{GGT} \left( h^{l-1}(t), \left\{ h^{l-1}(s) \mid s \in \mathcal{N}_{r_2}^l(t) \right\} \right), & (12) \end{cases}$$

where  $\mathcal{N}_{r_1}^l(t)$ ,  $\mathcal{N}_{r_2}^l(t)$  are node  $t$ 's neighbors of  $r_1$  and  $r_2$  relations, respectively.

For each video, the neighborhood messages carry information about the social influence of its *is\_followed\_by* neighbors. Since not all videos are created through imitation, in GGT we use a gated mechanism to filter irrelevant information for tackling Behavior Spread modeling challenge. For each tag  $t \in \mathcal{V}_{\text{tag}}$ , the neighborhood messages bring linguistic and visual knowledge from *is\_subtopic\_of* and *has\_tag* neighbors, respectively. Therefore, we propose AAN to solve the visual-linguistic aggregation challenge in the next stage.

In the *cross-relation message aggregation* stage, AAN is applied for tag nodes only to aggregate subtopic messages  $m_{r_1}^l(t)$  and video messages  $m_{r_2}^l(t)$ . For each tag  $t \in \mathcal{V}_{\text{tag}}$ , its representation is updated by:

$$h^l(t) = \text{AAN} \left( m_{r_1}^l(t), m_{r_2}^l(t) \right). \quad (13)$$

After updating node representations following the above two stages in each GNN layer, we get the final representation  $h^L$ .

**4.3.2 Gated Graph Transformer.** The goal of GGT is to derive a message information  $m_r^l(t) \in \mathbb{R}^d$  propagated from their neighbors in the ( $l$ )-th layer, where  $r$  is the neighbor relation. As illustrated in Fig. 4(a), we apply graph transformer to aggregate neighborhood information, and gated residual network to filter irrelevant information. Formally, we denote the central node as target  $t$  and neighbor node as source  $s \in \mathcal{N}_r^l(t)$ . The GGT is parameterized by target node type  $a_t$ , source node type  $a_s$ , and neighbor relation  $r$ .

Inspired by the Transformer architecture [8, 27], we first treat target node  $t$  as the query  $q_r^l(t) \in \mathbb{R}^d$ , and source nodes  $s \in \mathcal{N}_r^l(t)$

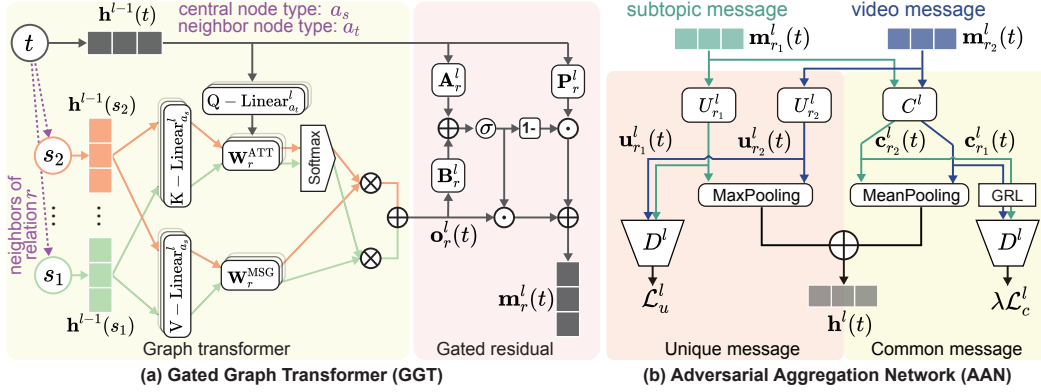


Figure 4: (a) GGT aggregates neighbor information using graph transformer, and filters irrelevant information using gated residual network. (b) ANN separates subtopic and video messages into common and unique information, and aggregates them.

as both keys  $k_r^l(s) \in \mathbb{R}^d$  and values  $v_r^l(s) \in \mathbb{R}^d$ :

$$\begin{cases} q_r^l(t) = Q\text{-Linear}_{a_t}^l(h^{l-1}(t)), & (14) \\ k_r^l(s) = K\text{-Linear}_{a_s}^l(h^{l-1}(s)), & (15) \\ v_r^l(s) = V\text{-Linear}_{a_s}^l(h^{l-1}(s)) W_r^{MSG}, & (16) \end{cases}$$

where  $Q\text{-Linear}_{a_t}^l$ ,  $K\text{-Linear}_{a_s}^l$ ,  $V\text{-Linear}_{a_s}^l$  are the linear transformation layers corresponding to specific node types, and  $W_r^{MSG} \in \mathbb{R}^{d \times d}$  is the message matrix of relation  $r$ .

Then, we calculate dot product between query and keys, and apply softmax to measure the importance of source node  $s$  with respect to target node  $t$  as  $\alpha_r^l(t, s) \in \mathbb{R}$ :

$$\alpha_r^l(t, s) = \frac{\exp(q_r^l(t) W_r^{ATT} k_r^l(s)^T / \sqrt{d})}{\sum_{w \in \mathcal{N}_r^l(t)} \exp(q_r^l(t) W_r^{ATT} k_r^l(w)^T / \sqrt{d})}, \quad (17)$$

where  $W_r^{ATT} \in \mathbb{R}^{d \times d}$  is an edge-based projection matrix. Note that the softmax is done within source nodes of the same relation  $r$ , and we name it separate attention. This is different from the mutual attention in the existing graph transformer [8] in which normalization is done within neighbors of all relations. We adopt separate attention because the different relations in the video-tag network are substantially different, and can not be weighed together.

Afterward, we can get the output of graph transformer  $o_r^l(t) \in \mathbb{R}^d$  by weighted summation of values:

$$o_r^l(t) = \sum_{s \in \mathcal{N}_r^l(t)} \alpha_r^l(t, s) v_r^l(s). \quad (18)$$

Finally, we propose the **gated residual network** to derive neighborhood message  $m_r^l(t)$ :

$$\begin{cases} z_r^l(t) = \text{Sigmoid}(A_r^l h^{l-1}(t) + B_r^l o_r^l(t)), & (19) \\ m_r^l(t) = z_r^l(t) \odot o_r^l(t) + (1 - z_r^l(t)) \odot (P_r^l h^{l-1}(t)), & (20) \end{cases}$$

where  $z_r^l(t) \in \mathbb{R}^d$  is the gating values,  $\odot$  denotes element-wise multiplication, and  $A_r^l, B_r^l, P_r^l \in \mathbb{R}^{d \times d}$  are linear transform matrices with respect to relation  $r$  in the  $(l)$ -th layer. The gated mechanism generally filters irrelevant information. For *is\_followed\_by*

neighbors, it suppresses neighbors when videos are created not from imitation. For *is\_subtopic\_of* neighbors, it keeps only general semantics as an abstraction of subtopic tags.

For simplicity, we omit GELU activation function after  $P_r^l$ , bias vector after  $A_r^l, B_r^l$ , and  $P_r^l$ , and superscript  $l$  in  $W_r^{MSG}$  and  $W_r^{ATT}$ .

**4.3.3 Adversarial Aggregation Network.** The AAN is designed only for tag nodes to aggregate linguistic and visual knowledge from subtopic message and video messages, respectively. Both messages can be divided into unique (exists in one), and common information (exists in both). Existing methods such as concatenation or attention mechanism [31] are sub-optimal due to the ignorance of the redundancy in common information. Concretely, concatenation duplicates the common information, and attention mechanism tends to overlook the unique information [13, 19].

In our AAN, we propose to separate common and unique information in order to remove the redundant information while keeping the complementary one. Formally, for each target tag node  $t \in \mathcal{V}_{\text{tag}}$ , the incoming messages  $m_{r_1}^l(t)$  and  $m_{r_2}^l(t)$  are first separated into common message  $c_{r_1}^l(t) \in \mathbb{R}^d$ ,  $c_{r_2}^l(t) \in \mathbb{R}^d$ :

$$\begin{cases} c_{r_1}^l(t) = C^l(m_{r_1}^l(t)), & (21) \\ c_{r_2}^l(t) = C^l(m_{r_2}^l(t)), & (22) \end{cases}$$

and unique message  $u_{r_1}^l(t), u_{r_2}^l(t)$ :

$$\begin{cases} u_{r_1}^l(t) = U_{r_1}^l(m_{r_1}^l(t)), & (23) \\ u_{r_2}^l(t) = U_{r_2}^l(m_{r_2}^l(t)), & (24) \end{cases}$$

where  $C^l(\cdot)$ ,  $U_{r_1}^l(\cdot)$  and  $U_{r_2}^l(\cdot)$  are linear transformation layers for learning common features, and unique features for the *is\_subtopic\_of* and *has\_tag* relation, respectively.

In order to ensure the above separation is successful, we need to keep the distributions of  $c_{r_1}^l(t), c_{r_2}^l(t)$  as close as possible, and those of  $u_{r_1}^l(t), u_{r_2}^l(t)$  as far as possible. There are two potential methods. One is to measure the distance between distributions using mutual information. Its drawback is that only the upper and lower bound of mutual information can be estimated. Thus, we adopt the other method, i.e., adversarial training, which is built

**Table 1: Dataset Statistics.**

Dataset	#Video	#Tag	#Tags	#Followers	#Videos	#Subtopics
			/Video		/Tag	
apparel	245,353	4,817	5.1	468.4	259.8	3.0
cosmetics	96,924	3,114	4.0	101.5	124.5	2.2
food	108,206	8,640	4.3	24.6	53.8	2.4

around a min-max game. A discriminator is used to distinguish two unique features  $u_{r_1}^l(t)$ ,  $u_{r_2}^l(t)$  while being confused about the common ones  $c_{r_1}^l(t)$ ,  $c_{r_2}^l(t)$ . Formally, we have:

$$\min_{D^l, U_{r_1}^l, U_{r_2}^l} \max_{C^l} \mathcal{L}_{adv}^l = \mathcal{L}_u^l + \lambda \mathcal{L}_c^l, \quad (25)$$

$$\begin{cases} \mathcal{L}_u^l = -\log \left( D^l \left( u_{r_1}^l(t) \right) \right) - \log \left( 1 - D^l \left( u_{r_2}^l(t) \right) \right), & (26) \\ \mathcal{L}_c^l = -\log \left( D^l \left( c_{r_1}^l(t) \right) \right) - \log \left( 1 - D^l \left( c_{r_2}^l(t) \right) \right), & (27) \end{cases}$$

where  $D^l$  is a binary linear classifier served as the discriminator,  $\lambda$  is a trade-off parameter, and  $\mathcal{L}_c^l$ ,  $\mathcal{L}_u^l$  are discrimination loss for common and unique features, respectively.

After common-unique separation, we directly aggregate them to derive the output representation  $h^l(t)$  for tag node  $t$ :

$$\begin{cases} c^l(t) = \text{MeanPool} \left( c_{r_1}^l(t) + c_{r_2}^l(t) \right), & (28) \\ u^l(t) = \text{MaxPool} \left( u_{r_1}^l(t) + u_{r_2}^l(t) \right), & (29) \\ h^l(t) = \frac{1}{2} \left( u^l(t) + c^l(t) \right). & (30) \end{cases}$$

**4.3.4 Training and Inference.** We compute the semantic similarity between a video and all tags as our predictions. Specifically, for each video node  $v$  and tag node  $t$ , the probability whether node  $v$  has tag  $t$  is estimated as  $\hat{s}(v, t) \in \mathbb{R}$ :

$$\hat{s}(v, t) = \text{Sigmoid} \left( h^L(v) \cdot \left( h^L(t) \right)^T \right). \quad (31)$$

During training, we apply the binary cross-entropy (BCE) loss  $L_{tag}$  as tagging loss:

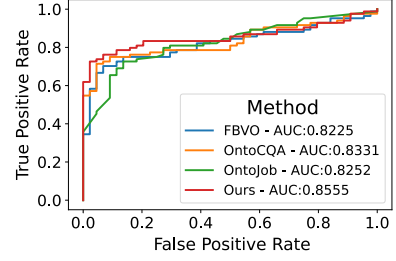
$$L_{tag} = \text{BCE} \left( y(v, t), \hat{s}(v, t) \right), \quad (32)$$

where  $y(v, t)$  is the ground truth for whether video  $v$  has tag  $t$ .

We use gradient reversal layer (GRL) [7] to implement the min-max game in Eqn. (25) for end-to-end training. The final loss  $L$  is composed of classification loss and adversarial training loss:

$$L = L_{tag} + \sum_{l=1}^L \mathcal{L}_{adv}^l. \quad (33)$$

During inference, a new video has no out-coming relations, because it has no tags (no *has\_tag* relations), and only previously-uploaded videos can influence the newly-uploaded ones (no out-coming *is\_followed\_by* relations). Hence the node representation of old nodes can be computed in advance. Thus, when a new video is added to the video-tag network, we only need to calculate its in-coming *is\_followed\_by* messages  $m_{r_3}^l(t)$  to get the video representation. Therefore, our model can achieve inductive inference.

**Figure 5: ROC of subtopic discovery**

## 5 EXPERIMENTS

### 5.1 Dataset

**5.1.1 Data Collection and Preparation.** We obtained a large-scale and real-world micro-video dataset from three verticals (apparel, cosmetics, and food) on Kuaishou platforms. We randomly selected 500,000 micro-videos on the featured page from July 14 to August 14, 2021. Their tags are obtained from a variety of human-based signals (e.g., query-watch) and the online video tagging system which leverages only video textual descriptions. The follow relations among video creators is collected on August 14, and we filtered robot users along with their videos. We excluded too short (< 1 sec) or too long (> 60 secs) micro-videos, removed the non-visual tags, and filtered videos with less than 2 tags.

To quantify the dataset quality, we manually evaluated 1000 randomly sampled micro-videos, and the tagging accuracy and recall is 91.3% and 66.2%, respectively. Our dataset is split into 3 partitions: train (80%), validate (10%), and test (10%).

**5.1.2 Tag Ontology Construction.** We constructed the tag ontology according to our proposed method in Section 4.1. We annotated 1,000 out of 768,798 co-occurred tag pairs. The two thresholds  $\delta_r$ ,  $\epsilon_r$  are defined according to the precision and recall of subtopic discovery. Concretely, we chose  $\delta_r$  where the precision is 90%, and  $\epsilon_r$  where the recall is 90%. As illustrated in Fig. 5, we measured the construction performance of subtopic discovery, and our method outperforms the rule-based method FBVO [6], unsupervised method OntoJob [29] and OntoCQA [26] in a clear margin. Our constructed ontology covers 96.67% of tags, and only 2.94% of tags are covered through  $\epsilon_r$  relaxation.

**5.1.3 Dataset Statistics.** We presented the statistics of our dataset in Table 1. Their diverged statistics lead to different results in the following experiments. The apparel dataset has the richest visual information (the #videos per tag), and the food dataset has the lowest social network and tag ontology density (the least #followers per video and the second least #subtopics per tag).

### 5.2 Experimental Settings

**5.2.1 Experimental Details.** The tag word embedding is derived from the last hidden layer of BERT. The video frame embedding is acquired from TSN backbone by SwinTransformer. In every GNN layer, we sample 4 neighbors for each type of relations following the practice of Deep Graph Library [30] because of the GPU memory limit. The number of layers  $L$  is set to 2. We set the batch size to be 1024, and used AdamW optimizer with a learning rate of 0.0005. We set feature and edge dropout to 0.2. Following Ganin and Lempitsky [7] to stabilize the adversarial training, we gradually changed  $\lambda$  from

**Table 2: Performance comparison with the baselines.**

Model	Apparel Dataset					Cosmetics Dataset					Food Dataset				
	mAP	P@1	P@3	R@5	R@10	mAP	P@1	P@3	R@5	R@10	mAP	P@1	P@3	R@5	R@10
Vanilla	59.89	89.22	74.97	57.12	64.68	46.33	74.30	45.49	47.23	56.06	45.98	60.13	47.78	50.57	59.60
ML-GCN	61.49	91.24	76.75	57.97	65.53	48.03	77.20	46.42	48.15	57.02	47.54	63.94	49.65	51.75	59.97
NeXtVLAD	63.14	91.90	77.44	58.86	66.98	49.78	77.93	47.93	49.58	58.92	48.49	64.92	50.51	52.43	60.93
CMA	63.04	91.51	77.29	58.85	66.99	50.24	78.60	48.29	50.04	59.41	49.28	65.54	50.91	53.09	61.65
MALL-CNN	63.31	91.67	77.95	59.07	67.20	50.46	78.93	48.25	50.15	59.83	49.58	66.00	50.89	53.32	61.99
TagGNN	63.44	93.15	78.23	59.13	66.82	52.39	84.80	50.32	51.64	60.37	50.92	74.49	53.58	53.09	60.05
HAN	61.83	92.17	77.06	58.00	65.76	51.72	84.87	49.54	51.31	59.99	50.76	75.32	53.53	53.02	59.79
HGT	63.85	92.35	78.25	59.43	67.58	54.50	86.62	51.78	53.61	62.62	51.56	76.22	54.38	53.53	60.04
SimpleHGN	63.16	91.80	77.99	59.09	67.10	53.68	86.28	51.17	52.80	61.62	52.76	77.27	55.21	54.19	61.33
<b>Ours</b>	<b>65.05</b>	<b>93.74</b>	<b>79.07</b>	<b>59.89</b>	<b>68.22</b>	<b>56.55</b>	<b>88.16</b>	<b>53.18</b>	<b>54.98</b>	<b>64.55</b>	<b>56.93</b>	<b>82.16</b>	<b>58.94</b>	<b>57.11</b>	<b>63.99</b>

0 to  $\lambda_0$  according to the schedule:  $\lambda = \lambda_0 (2 / (1 + \exp(-\gamma p)) - 1)$ , where  $p$  linearly changes from 0 to 1 in the training process. The  $\gamma$  and  $\lambda_0$  was set to 20 and 0.0005 for all datasets, respectively. All the settings are applied equally to all baseline methods.

**5.2.2 Evaluation Metrics.** We adopted three common metrics for multi-label classification: mean Average Precision (mAP), Precision@K (P@K), and Recall@K (R@K). The P@K and R@K measure the tagging performance of top K tags, while mAP measures the overall ranking results of all tags.

### 5.3 Baselines

In order to verify our RADAR model, we compared it with the following baselines:

- Video tagging methods: ML-GCN [3], NeXtVLAD [15, 36], CMA [38], and MALL-CNN [14]. We compared them to demonstrate the effectiveness of incorporating extra social networks and tag graph information. Note that NeXtVLAD, CMA, and MALL-CNN have sequence-level feature  $h \in \mathbb{R}^{F \times d}$  as input, with an extra aggregation module instead of meaning pooling in our method.
- Heterogeneous GNN methods: HAN [31], TagGNN [21], HGT [8], and Simple-HGN [20] are four representative methods on heterogeneous GNN, and Simple-HGN is the state-of-the-art. We compared our RADAR with them to demonstrate the effectiveness of our RADAR model.

### 5.4 Performance Comparison

Compared with baselines, our results are summarized in Table 2. By analyzing this table, we gained the following observations:

- The heterogeneous GNN methods generally outperform the video tagging baselines. Their main difference is that tagging baselines better leverage video frame features, and GNN methods leverage tag ontology and extra social network. The improvement indicates that for micro-videos, incorporating social influence and tag relations is more effective than modeling frame features.
- Our proposed model RADAR outperforms all heterogeneous GNN methods consistently. Compared with the best-performing baselines, RADAR obtains relative mAP gains with 1.9% in Apparel, 3.8% in Cosmetics, and 7.9% in Food dataset. The improvement demonstrates the superiority of RADAR in video tagging.
- Simple-HGN is the only heterogeneous GNN baseline whose relevant rank differs among datasets. Notably, its performance is the

best in Food while the second-worst in Apparel dataset within all heterogeneous GNN baselines. Coincidentally, this relevant rank is opposite to the datasets’ social network and tag ontology density. The denser *is\_followed\_by* and *is\_subtopic\_of* relations are, the worse Simple-HGN performs. Considering that Simple-HGN is the start-of-the-art method for general heterogeneous GNN, we attributed this phenomenon to the fact that video tagging is quite different from the previous tasks. In video tagging, The video feature from frames and tag feature from language models are two modalities with large semantic gaps. This phenomenon also demonstrates the necessity of our adversarial aggregation network which aggregates the visual and linguistic information.

### 5.5 Ablation Studies

In this section, we carried out several experiments to further analyze the effectiveness of our model, as reported in Table 3. Concretely, we first explored the contributions of different relations in the video-tag network. We then analyzed the effectiveness of each component including Gated Graph Transformer (GGT) and Adversarial Aggregation Network (AAN).

**5.5.1 Ablation of different relations.** We compared our model with the following variants: 1) **w/o followed by**, removing *is\_followed\_by* relations; 2) **w/o subtopic**, removing *is\_subtopic\_of* relations; and 3) **w/o subtopic & followed by**, removing both relations.

The result of **w/o followed by** is consistently lower than of **w/o subtopic** in three datasets, suggesting that the social network information contributes more than tag ontology.

Note that if we remove *is\_followed\_by* from our full model, the performance drop is more significant than we remove *is\_followed\_by* from **w/o subtopic**. In another view, the addition of *is\_followed\_by* relations will bring larger improvement when the *is\_subtopic\_of* relations exist. Therefore, the combination of the two relations is not the naive summation of the two relations. This is evidence that the two relations have complementary information, and thus the separation of common and unique information in the AAN module is necessary.

**5.5.2 Ablation of GGT.** We replaced the gated residual network in GGT with a residual network to be the variant **w/o gated residual**, and replaced the separate attention with mutual attention to be the variant **w/ mutual attention**. Compared with our full model, the performance of **w/o gated residual** and **w/ mutual attention**

**Table 3: Ablation study on the effectiveness of the two relations, gated graph transformer, and adversarial aggregation network.**

Model	Apparel Dataset					Cosmetics Dataset					Food Dataset				
	mAP	P@1	P@3	R@5	R@10	mAP	P@1	P@3	R@5	R@10	mAP	P@1	P@3	R@5	R@10
w/o followedby	62.28	91.49	76.97	58.49	66.34	48.68	77.71	47.11	48.72	58.00	47.37	63.89	49.87	51.78	60.26
w/o subtopic	63.60	93.56	78.43	59.17	66.96	53.17	86.23	50.93	52.43	60.98	53.27	79.39	56.37	54.67	60.74
w/o subtopic & followedby	62.17	91.45	76.97	58.39	66.18	48.33	77.35	46.88	48.59	57.57	46.48	63.33	48.82	51.38	59.35
w/o gated residual	64.20	93.32	78.54	59.52	67.66	55.20	86.77	52.06	54.06	63.27	55.65	80.90	57.74	56.18	62.94
w/ mutual attention	64.12	93.34	78.55	59.44	67.61	55.32	87.35	52.14	54.10	63.35	55.69	81.00	57.66	56.34	63.24
w/ concatenation	63.82	93.34	78.50	59.24	67.16	53.48	86.57	51.20	52.58	61.32	52.64	78.25	55.67	54.20	60.50
w/ attention	64.76	93.48	78.97	59.78	67.89	55.27	88.01	52.30	53.89	62.86	55.47	81.64	58.13	56.11	62.45
w/ LMF	64.36	93.25	78.98	59.63	67.72	55.00	87.51	52.25	53.67	62.42	54.85	81.24	57.64	55.69	61.71
w/o $L_{adv}$	63.87	93.21	78.60	59.38	67.28	54.31	86.57	51.83	53.47	62.26	56.57	82.08	58.78	56.88	63.44
w/ bidirectional edges	65.26	93.94	79.13	60.09	68.35	56.86	88.06	53.34	55.12	64.65	57.19	82.27	58.98	57.35	64.32
Ours	65.05	93.74	79.07	59.89	68.22	56.55	88.16	53.18	54.98	64.55	56.93	82.16	58.94	57.11	63.99

consistently dropped in all datasets. This indicates that it is important to filter irrelevant information for modeling Behavior Spread, and separate attention is a useful design under the modality gap.

**5.5.3 Ablation of AAN.** To validate the impact of our proposed AAN, we conducted a series of experiments by introducing four variants: 1) **w/ concatenation**, replacing AAN with vector concatenation and a linear transformation layer, which is the simplest multi-modal aggregation method; 2) **w/ attention**, replacing AAN with attention module in [31]; 3) **w/ LMF**, replacing AAN with Low-rank Multi-modal Fusion (LMF) [18], which is the best multi-modal vector aggregation method; and 4) **w/o  $L_{adv}$** , removing the adversarial loss  $L_{adv}$ .

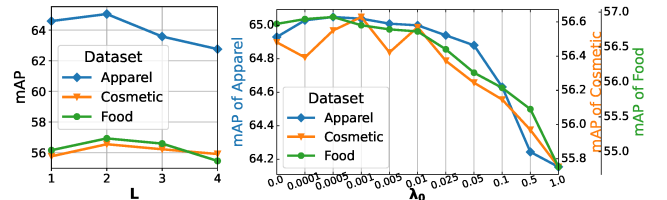
From Table 3, we observed that our method outperforms all the multi-modal vector aggregation methods consistently. The improvement is not owing to the increased parameters, because **w/ LMF** has the most parameters. Compared with **w/o  $L_{adv}$** , we attributed the improvement to the separation of common and unique information in the visual and linguistic messages.

**5.5.4 Bidirectional edges.** We also explored the effect of bidirectional edges. Specifically, in the variant **w/ bidirectional edges**, we added *is\_supertopic\_of* and *has\_video* relations to the network. We also applied AAN to video nodes since they have two types of inbound messages. Note that we did not add *follows* relations, because we hope the new videos do not send messages to the original graph for inductive learning. Although this variant slightly improves the performance, we do not adopt this setting considering the extra computational burden.

## 5.6 Sensitivity Analysis

We investigated how different choices of hyper-parameters affect performance. We explored two main parameters: the number of GNN layer  $L$  and the maximal weight of unique loss  $\lambda_0$ .

As illustrated in Fig. 6, our model performs best when it has two GNN layers, which is common in graph neural networks due to over-smoothing. Our model achieves the best performance when  $\lambda_0$  is around 0.0005 to 0.001, which indicates an appropriate balance between unique and common loss. Note that  $\lambda_0 = 0$  is different from **w/o  $L_{adv}$** . Although both of them have no common information, the discriminator  $D^I$  in the latter variant is removed, so it has no unique information as well. We observed that **w/o  $L_{adv}$**  will cause

**Figure 6: Sensitivity analysis**

a larger performance drop compared with setting  $\lambda_0 = 0$ . This indicates that the unique information is more important.

## 6 CONCLUSION AND FUTURE WORK

In this work, we jointly incorporate social influence and tag relations into a user-video-tag network to enhance micro-video tagging. To construct tag relations, we build a tag ontology based upon tag statistics and graphical constraints in a semi-supervised manner. To derive a better node representation in video-tag network, we present RADAR, a heterogeneous GNN composed of a gated graph transformer and adversarial aggregation network. Extensive experimental results on three datasets have demonstrated the superiority of RADAR, and the effectiveness of its two components.

In the future, we are going to generalize our method to handle more complicated tag knowledge structures. As to the Behavior Spread modeling, we plan to model the temporal dynamics of users' social influence.

## 7 ACKNOWLEDGEMENTS

This work is supported by the National Natural Science Foundation of China, No.: 62176137, No.:U1936203, and No.: 62006140; the Shandong Provincial Natural Science and Foundation, No.: ZR2020QF106; Beijing Academy of Artificial Intelligence(BAAI); Kuaishou Technology.



## REFERENCES

- [1] Damon Centola. 2010. The Spread of Behavior in an Online Social Network Experiment. *Science* 329 (2010), 1194–1197.
- [2] Xu Chen, Changying Du, Xiuqiang He, and Jun Wang. 2020. JIT2R: A Joint Framework for Item Tagging and Tag-based Recommendation. In *Proceedings of the International ACM SIGIR Conference on Research and Development in Information Retrieval*. ACM, 1681–1684.
- [3] Zhao-Min Chen, Xiu-Shen Wei, Peng Wang, and Yanwen Guo. 2019. Multi-Label Image Recognition With Graph Convolutional Networks. In *Proceedings of the IEEE Conference on Computer Vision and Pattern Recognition*. IEEE, 5177–5186.
- [4] Ali Diba, Mohsen Fayyaz, Vivek Sharma, Manohar Paluri, Jürgen Gall, Rainer Stiefelhagen, and Luc Van Gool. 2020. Large Scale Holistic Video Understanding. In *Proceedings of the European Conference on Computer Vision*. Springer, 593–610.
- [5] Yujie Fan, Mingxuan Ju, Shifu Hou, Yanfang Ye, Wenqiang Wan, Kui Wang, Yinming Mei, and Qi Xiong. 2021. Heterogeneous Temporal Graph Transformer: An Intelligent System for Evolving Android Malware Detection. In *Proceedings of the ACM SIGKDD Conference on Knowledge Discovery and Data Mining*. ACM, 2831–2839.
- [6] Quan Fang, Changsheng Xu, Jitao Sang, M. Shamim Hossain, and Ahmed Ghoneim. 2016. Folksonomy-Based Visual Ontology Construction and Its Applications. *IEEE Transactions on Multimedia* 18 (2016), 702–713.
- [7] Yaroslav Ganin and Victor S. Lempitsky. 2015. Unsupervised Domain Adaptation by Backpropagation. In *Proceedings of the International Conference on Machine Learning*. JMLR.org, 1180–1189.
- [8] Ziniu Hu, Yuxiao Dong, Kuansan Wang, and Yizhou Sun. 2020. Heterogeneous Graph Transformer. In *Proceedings of the International World Wide Web Conference*. ACM, 2704–2710.
- [9] Di Jin, Zhongang Qi, Yingmin Luo, and Ying Shan. 2021. TransFusion: Multimodal Fusion for Video Tag Inference via Translation-based Knowledge Embedding. In *Proceedings of the ACM International Conference on Multimedia*. ACM, 1093–1101.
- [10] Denis Kotkov, Alexandr Maslov, and Mats Neovius. 2021. Revisiting the Tag Relevance Prediction Problem. In *Proceedings of the International ACM SIGIR Conference on Research and Development in Information Retrieval*. ACM, 1768–1772.
- [11] Mengmeng Li, Tian Gan, Meng Liu, Zhiyong Cheng, Jianhua Yin, and Liqiang Nie. 2019. Long-tail Hashtag Recommendation for Micro-videos with Graph Convolutional Network. In *Proceedings of the ACM International Conference on Information and Knowledge Management*. ACM, 509–518.
- [12] Xirong Li, Shuai Liao, Weiyu Lan, Xiaoyong Du, and Gang Yang. 2015. Zero-shot Image Tagging by Hierarchical Semantic Embedding. In *Proceedings of the International ACM SIGIR Conference on Research and Development in Information Retrieval*. ACM, 879–882.
- [13] Xiang Li, Chao Wang, Jiwei Tan, Xiaoyi Zeng, Dan Ou, and Bo Zheng. 2020. Adversarial Multimodal Representation Learning for Click-Through Rate Prediction. In *Proceedings of the International World Wide Web Conference*. ACM, 827–836.
- [14] Xuewei Li, Hongjun Wu, Mengzhu Li, and Hongzhe Liu. 2022. Multi-label video classification via coupling attentional multiple instance learning with label relation graph. *Pattern Recognition Letters* 156 (2022), 53–59.
- [15] Rongcheng Lin, Jing Xiao, and Jianping Fan. 2018. NeXtVLAD: An Efficient Neural Network to Aggregate Frame-Level Features for Large-Scale Video Classification. In *Proceedings of the European Conference on Computer Vision Workshops*. Springer, 206–218.
- [16] Bang Liu, Weidong Guo, Di Niu, Chaoyue Wang, Shunnan Xu, Jinghong Lin, Kunfeng Lai, and Yu Xu. 2019. A User-Centered Concept Mining System for Query and Document Understanding at Tencent. In *Proceedings of the ACM SIGKDD International Conference on Knowledge Discovery & Data Mining*. ACM, 1831–1841.
- [17] Can Liu, Li Sun, Xiang Ao, Jinghua Feng, Qing He, and Hao Yang. 2021. Intention-aware Heterogeneous Graph Attention Networks for Fraud Transactions Detection. In *Proceedings of the ACM SIGKDD Conference on Knowledge Discovery & Data Mining*. ACM, 3280–3288.
- [18] Zhun Liu, Ying Shen, Varun Bharadhwaj Lakshminarasimhan, Paul Pu Liang, Amir Zadeh, and Louis-Philippe Morency. 2018. Efficient Low-rank Multimodal Fusion With Modality-Specific Factors. In *Proceedings of the Annual Meeting of the Association for Computational Linguistics*. ACL, 2247–2256.
- [19] Yan Lu, Yue Wu, Bin Liu, Tianzhu Zhang, Baopu Li, Qi Chu, and Nenghai Yu. 2020. Cross-Modality Person Re-Identification With Shared-Specific Feature Transfer. In *Proceedings of the IEEE Conference on Computer Vision and Pattern Recognition*. IEEE, 13376–13386.
- [20] Qingsong Lv, Ming Ding, Qiang Liu, Yuxiang Chen, Wenzheng Feng, Siming He, Chang Zhou, Jianguo Jiang, Yuxiao Dong, and Jie Tang. 2021. Are we really making much progress?: Revisiting, benchmarking and refining heterogeneous graph neural networks. In *Proceedings of the ACM SIGKDD Conference on Knowledge Discovery & Data Mining*. ACM, 1150–1160.
- [21] Kelong Mao, Xi Xiao, Jieming Zhu, Biao Lu, Ruiming Tang, and Xiuqiang He. 2020. Item Tagging for Information Retrieval: A Tripartite Graph Neural Network based Approach. In *Proceedings of the International ACM SIGIR Conference on Research and Development in Information Retrieval*. ACM, 2327–2336.
- [22] Liqiang Nie, Yongqi Li, Fuli Feng, Xuemeng Song, Meng Wang, and Yinglong Wang. 2020. Large-Scale Question Tagging via Joint Question-Topic Embedding Learning. *ACM Transactions on Information Systems* 38 (2020), 20:1–20:23.
- [23] Jingbo Shang, Jialu Liu, Meng Jiang, Xiang Ren, Clare R. Voss, and Jiawei Han. 2018. Automated Phrase Mining from Massive Text Corpora. *IEEE Transactions on Knowledge and Data Engineering* 30 (2018), 1825–1837.
- [24] Si Sun, Zhenghao Liu, Chenyan Xiong, Zhiyuan Liu, and Jie Bao. 2021. Capturing Global Informativeness in Open Domain Keyphrase Extraction. In *Proceedings of the Natural Language Processing and Chinese Computing*. Springer, 275–287.
- [25] Teng Sun, Chun Wang, Xuemeng Song, Fuli Feng, and Liqiang Nie. 2022. Response Generation by Jointly Modeling Personalized Linguistic Styles and Emotions. *ACM Transactions on Multimedia Computing, Communications, and Applications (TOMM)* 18 (2022), 1–20.
- [26] K. Suryamukhi, P. D. Vivekananda, and Manish Singh. 2021. Mining Tag Relationships in CQA Sites. In *Conceptual Modeling - International Conference, ER*. Springer, 345–355.
- [27] Ashish Vaswani, Noam Shazeer, Niki Parmar, Jakob Uszkoreit, Llion Jones, Aidan N. Gomez, Lukasz Kaiser, and Illia Polosukhin. 2017. Attention is All you Need. In *Proceedings of the Neural Information Processing Systems Conference*. MIT Press, 5998–6008.
- [28] Sunny Verma, Chen Wang, Liming Zhu, and Wei Liu. 2019. DeepCU: Integrating both Common and Unique Latent Information for Multimodal Sentiment Analysis. In *Proceedings of the International Joint Conference on Artificial Intelligence*. ijcai.org, 3627–3634.
- [29] Jarno Vrolijk, Stefan T. Mol, Christian Weber, Mohammadreza Tavakoli, Gabor Kismihok, and Mauro Pelucchi. 2022. OntoJob: Automated Ontology Learning from Labor Market Data. In *International Conference on Semantic Computing (ICSC)*. IEEE, 195–200.
- [30] Minjie Wang, Da Zheng, Zihao Ye, Quan Gan, Mufei Li, Xiang Song, Jinjing Zhou, Chao Ma, Lingfan Yu, Yu Gai, Tianjun Xiao, Tong He, George Karypis, Jinyang Li, and Zheng Zhang. 2019. Deep Graph Library: A Graph-Centric, Highly-Performant Package for Graph Neural Networks. *arXiv preprint arXiv:1909.01315* (2019).
- [31] Xiao Wang, Houye Ji, Chuan Shi, Bai Wang, Yanfang Ye, Peng Cui, and Philip S. Yu. 2019. Heterogeneous Graph Attention Network. In *Proceedings of the International World Wide Web Conference*. ACM, 2022–2032.
- [32] Ya Wang, Dongliang He, Fu Li, Xiang Long, Zhichao Zhou, Jinwen Ma, and Shilei Wen. 2020. Multi-Label Classification with Label Graph Superimposing. In *Proceedings of the AAAI Conference on Artificial Intelligence*. AAAI Press, 12265–12272.
- [33] Yinwei Wei, Zhiyong Cheng, Xuzheng Yu, Zhou Zhao, Lei Zhu, and Liqiang Nie. 2019. Personalized Hashtag Recommendation for Micro-videos. In *Proceedings of the ACM International Conference on Multimedia*. ACM, 1446–1454.
- [34] Yinwei Wei, Xiang Wang, Weili Guan, Liqiang Nie, Zhouchen Lin, and Baoquan Chen. 2019. Neural Multimodal Cooperative Learning toward Micro-video Understanding. *IEEE Transactions on Image Processing* 29 (2019), 1–14.
- [35] Yinwei Wei, Xiang Wang, Liqiang Nie, Xiangnan He, and Tat-Seng Chua. 2020. Graph-refined Convolutional Network for Multimedia Recommendation with Implicit Feedback. In *Proceedings of the 28th ACM international conference on multimedia*. ACM, 3541–3549.
- [36] Hao Wu, Jiajie Wang, Yuanzhe Gu, Peisen Zhao, and Zhonglin Zu. 2021. A Solution to Multi-modal Ads Video Tagging Challenge. In *Proceedings of the ACM International Conference on Multimedia*. ACM, 4808–4812.
- [37] Wenmain Yang, Kun Wang, Na Ruan, Wenyan Gao, Weijia Jia, Wei Zhao, Nan Liu, and Yunyong Zhang. 2019. Time-Sync Video Tag Extraction Using Semantic Association Graph. *ACM Transactions on Knowledge Discovery from Data* 13 (2019), 37:1–37:24.
- [38] Renchun You, Zhiyao Guo, Lei Cui, Xiang Long, Yingze Bao, and Shilei Wen. 2020. Cross-Modality Attention with Semantic Graph Embedding for Multi-Label Classification. In *Proceedings of the AAAI Conference on Artificial Intelligence*. AAAI Press, 12709–12716.
- [39] Le Zhang, Ding Zhou, Hengshu Zhu, Tong Xu, Rui Zha, Enhong Chen, and Hui Xiong. 2021. Attentive Heterogeneous Graph Embedding for Job Mobility Prediction. In *Proceedings of the ACM SIGKDD Conference on Knowledge Discovery & Data Mining*. ACM, 2192–2201.
- [40] Shengming Zhang, Hao Zhong, Zixuan Yuan, and Hui Xiong. 2021. Scalable Heterogeneous Graph Neural Networks for Predicting High-potential Early-stage Startups. In *Proceedings of the ACM SIGKDD Conference on Knowledge Discovery & Data Mining*. ACM, 2202–2211.